

## **INSIDIA: a FIJI Macro Delivering High-throughput and High-content Spheroid Invasion Analysis**

Chiara Moriconi<sup>1\*</sup>, Valentina Palmieri<sup>2,3\*</sup>, Riccardo di Santo<sup>2</sup>, Giusy Tornillo<sup>4</sup>,  
Massimiliano Papi<sup>2,3</sup>, Geoff Pilkington<sup>5</sup>, Marco De Spirito<sup>2</sup>, Mark Gumbleton<sup>1</sup>

<sup>1</sup>School of Pharmacy and Pharmaceutical Sciences, Cardiff University, UK, <sup>2</sup>Physics Institute, Catholic University of Sacred Heart, Rome, Italy, <sup>3</sup>Institute for Complex Systems, National Research Council (CNR), Rome, Italy, <sup>4</sup>European Cancer Stem Cell Research Institute, Cardiff University, UK, <sup>5</sup>Institute of Biomedical and Biomolecular Science, School of Pharmacy and Biomedical Sciences, University of Portsmouth, UK

\* These authors contributed equally to the present work.

**Correspondence:** Professor Mark Gumbleton, Cardiff University, CF10 3NB, Cardiff, UK.

**E-mail:** [Gumbleton@cardiff.ac.uk](mailto:Gumbleton@cardiff.ac.uk)

**Keywords:** Spheroid, core, invasion, FIJI, quantitation, analysis

**Abbreviations:** CT - Core-Thresholding; INSIDIA - INvasion Spheroid Imagej Analysis; Maxradius - Maximum Radius; SS - Spheroid-Segmentation.

**Abstract**

Time-series image capture of in-vitro 3D spheroidal cancer models embedded within an extracellular matrix affords examination of spheroid growth and cancer cell invasion. However, a customisable, comprehensive and open source solution for the quantitative analysis of such spheroid images is lacking. Here, we describe INSIDIA (INvasion Spheroid ImageJ Analysis), an open-source macro implemented as a customisable software algorithm running on the FIJI platform, that enables high-throughput high-content quantitative analysis of spheroid images (both bright-field grey and fluorescent images) with the output of a range of parameters defining the spheroid 'tumour' core and its invasive characteristics.

## **1 Introduction**

The in-vitro study of cancer cell invasion increasingly exploits 3D spheroidal models of cancer cells or tumour organoids embedded within an extracellular matrix (ECM)<sup>1</sup>. Such models accommodate many relevant biological characteristics including different patterns of spheroid core growth and cell invasion into the surrounding ECM<sup>2,3</sup>. The 3D spheroid-sprouting assay<sup>4,5</sup> is one such relatively simple widely-used model whose changing phenotype is captured by time-series images, which can be either fluorescent or bright-field but with the latter more common and also presenting a greater challenge for image quantitation. Quantitation of images capturing the biological behavior of spheroids is generally, but not exclusively, limited to basic geometrical parameters, such as overall area or radius occupied by the expanding cellular mass<sup>6-8</sup>. While useful such information alone under-powers the potential of the spheroid assay. In particular, very few image analysis algorithms are capable of distinguishing spheroid 'Core' (i.e. the original cellular mass that may have undergone varying extents of proliferation) and the spheroid 'Invasive Edge' (representing motile cells invading the ECM). With this delineation comes the potential for a wider range of multi-parametric analyses related to spheroid malignancy<sup>12,13</sup>.

While image analysis software capable of detailed quantitative analysis of 3D spheroid assays is available, it is mostly licensed for a particular microscope platform, or is limited in calculable parameters and not customisable by the end-user (Table1). This current work describes an open-source customisable macro implemented to run on the FIJI<sup>15</sup> platform that enables rapid high-throughput and high-content quantitative analysis of spheroid images datasets. This macro, INSIDIA (INvasion Spheroid ID ImageJ Analysis) isolates the entire spheroid cellular mass from the image background with several user-options able to address poorly-contrasted images. In subsequent steps, INSIDIA distinguishes the spheroid core from the invasive edge and provides quantitative information describing growth and invasive behaviour. INSIDIA is easily implementable for both fluorescent and bright-field grey images.

## **2 Materials and Methods**

### **2.1 Cell lines and treatments**

The human, low passage glioblastoma cell line UP007 was established in culture at the University of Portsmouth from biopsy tissue (71 year old male Kings College Hospital London ethics permission, 11/SC/0048). Spheroid invasion behaviour of UP007 was modified by the dual Src/Abl tyrosine-kinase inhibitor, Saracatinib

(SelleckChem, Houston, USA). Saracatinib was added to the spheroid cultures at DAY -(minus)1 achieving final concentrations of 0.5  $\mu$ M or 1 $\mu$ M per well. Control treatments received matched solvent.

Human glioblastoma cell line U87MG was obtained from ECACC (Porton Down, UK) with spheroid proliferation and invasive behaviour modified by Lentiviral transfection with shRNA targeting caveolin-1, with control using a non-target (NT) shRNA sequence. The culture medium for the glioma cell lines was DMEM 10% foetal bovine serum, 2% penicillin-streptomycin with cells maintained at 37°C in a humidified atmosphere of 5%CO<sub>2</sub>. Unless specifically identified all other general materials and plasticware were from Gibco-ThermoFisher (UK) Corning Life Sciences (UK) or Fisher Scientific (UK).

## **2.2 3D-Spheroid-sprouting assay and image capture.**

The spheroid-sprouting assay was conducted as previously described<sup>5</sup>. Briefly, at a defined time, i.e. DAY -(minus)4 2000 cells were seeded into each well of a 96-well ultra-low-adherence (ULA) round-bottomed plate (Figure 1A). Immediately, the plates were centrifuged (300g 1 min) forming a suspended loose cell aggregate. After four days (i.e. DAY 0) in suspension culture tight spheroidal cell aggregates had formed, at which point a 50% volume of medium was removed and replaced with an equal volume of 100% Matrigel™ (BD Biosciences, Oxford, UK) whereupon matrix-gel solidification progressed (1 hr 37°C). Over subsequent days (i.e. Day +1 to +4) spheroid growth and invasion was captured by bright-field microscopy (grey-scale images, Leica DMI1 microscope, MC170 HD camera 1024x786 pixel resolution).

## **2.3 Image analysis by INSIDIA macro**

Grey-scale images were organised into the required file structure for automatic batch processing. The principles of INSIDIA workflow are summarised in Figure 1 with each step discussed in detail in the 'Results and Discussion' section below; full operational details are provided in the "INSIDIA Guide".

The INSIDIA macro can be downloaded from: <https://valentinapalmieri.wixsite.com/insidia> together with the 'INSIDIA Guide' for users, test images and tutorial video.

## **3 Results & Discussion**

INSIDIA analyses is based on three sequential steps: (i) 'Spheroid-Segmentation'; (ii) 'Density-Profile/Core-Thresholding', and (iii) 'Density Map' analyses. Each provides quantitative metrics defining the change in spheroid characteristics across captured time-series images.

**3.1 Spheroid-Segmentation** (Figure 1B and 1C) comprises a set of morphological operations which isolate the spheroid cellular mass from the image background. The output is a binary image where the spheroid mass has an intensity of 255 (white pixels) and the background an intensity of 0 (black pixels). The delineated 'spheroid mask' or outline defines the image elements subjected to analysis in later steps of INSIDIA.

Isolating a spheroid's cellular material from an image background is especially difficult for greyscale images as the contrast can be low<sup>16</sup>, and can be further compromised by cell debris or defects in plasticware. To address this, while also allowing user-flexibility, INSIDIA has two options for 'Spheroid-Segmentation'; namely 'Image Thresholding', in manual or automatic modes, and 'Frangi-Filtering'<sup>17</sup>. With 'Image Thresholding' individual pixels are marked as 'object pixels' (i.e. not background) if their intensity value is equal to or greater than a set threshold value<sup>18</sup>. The threshold value may be determined automatically by FIJI within the '*Auto-Threshold tool*' built into INSIDIA or can be set manually by the user; the appropriateness of any threshold setting can be confirmed by the user through iterative reprocessing.

Nevertheless 'Spheroid-Segmentation' may be compromised by low pixel intensities with poor contrast to background, e.g. at the periphery of the spheroid mass cells may be migrating as part of invading edge (red arrows in Figure 1C). Here, a further option for 'Spheroid-Segmentation' is provided by 'Frangi-Filtering'<sup>17 19</sup> which has previously been used in the analyses of invasive edges by Blacher and colleagues<sup>11</sup>. INSIDIA applies the 'Frangi Filter' through the '*Frangi vesselness*' plugin within FIJI after first providing a set of parameters to optimize the edge detection; Figures 1B and 1C show representative comparisons of the same spheroid image mapped by either 'Image Thresholding' manual mode or by 'Frangi-Filtering'. Irrespective of the method for 'Spheroid-Segmentation' once the edges of the spheroid mass are identified the INSIDIA macro assigns a pixel intensity of 255 (white) to all the enclosed pixels creating a 'spheroid mask' or outline. Small white objects, noise in the image, may remain but INSIDIA eliminates these through the '*Analyse Particle*' tool to leave only the largest particle (the spheroid) in the binary image output.

The 'Spheroid-Segmentation' step also provides certain quantitative parameters for the user including: Centre of the Spheroid Mass, Maximum Radius, Total Area and Perimeter, as well as a number of secondary parameters, amongst others: Circularity and Shape Factor (functions of the Area and Perimeter parameters); Specific Surface (a measure of surface irregularity or roughness)<sup>9</sup>; Envelope Area (area of smallest convex polygon that encompasses the entire spheroid mass); INSIDIA Guide provides a complete list of parameter outputs.

**3.2 'Density-Profile/Core-Thresholding'** (Figures 1D to 1G) is a single step distinguishing a spheroid's core from the invasive edge.

An approach previously advocated to distinguish the spheroid core and invasive edge regions is simply a user-observed manual definition of the invasive region without reference to digital data, a method that has particular bias and not readily applicable for high throughput analyses<sup>10</sup>. An advance was made by Stein and colleagues<sup>9</sup> who scaled the pixels in spheroid mass between between 0 (the darkest pixel) to 1 (the lightest pixel), and defined those pixels with an intensity of less than 0.12 as representing the core. Again, the pixel threshold was based on user-defined observations of invasive behaviour which may not be useful for cells of differing characteristics, nor does it account for variable illumination conditions between the captured images, all of which promote bias in the 'image normalisation' process (see below). Finally, Blacher and colleagues<sup>11</sup> defined the interface between the spheroid core and the invading edge by tracing the largest inscribed circle in the spheroid mass that encompassed the 'core'. This method is influenced by the particular approach used for Spheroid-Segmentation, i.e, ability to distinguish the precise outline of the invading edge and also by the fact that a spheroid core is not always a perfect circle, for example the varying extents to which the invading edge protrusions return to the main cellular mass.

The 'Density-Profile/Core-Thresholding' step in INSIDIA involves:

1. Image-Normalisation - whereby all images are normalised to account for any changed illumination settings/conditions during the capture of time-series images. Here image background (average intensity of image pixels outside the spheroid mass) is subtracted from the digital data for the spheroid mass itself, and as such avoids the bias when normalisation is based on the darkest to lightest pixels alone.

2. Density-Profiling - implemented in a similar manner to that of Blacher et al<sup>11</sup>. Essentially, beginning at the spheroid's geometric centre of mass a series of concentric circular profiles (progressing in 1-pixel steps) are mapped to the spheroid image (Figure 1D) and ending at the point of maximum radius of the spheroid mass (identified at 'Spheroid-Segmentation' step). The average pixel density along each circular profile is plotted against the distance from the spheroid's centre generating a Density-Profile plot (Figure 1E). The plateau at early time points in the Profile corresponds to the uniform darker pixel intensity within the spheroid core. Moving away from the core the pixel intensity decreases most evident around the core - invasive edge boundary.

3. Core-Thresholding - automatically computed as the Density-Profile is generated, and defines the boundary value (CT-value) between a spheroid's core and invasive edges. For Day 0 spheroids, i.e. before invasion is evident, the core boundary is synonymous with the high contrast interface of the cells with the ECM and the subsequent Density-Profile will display an almost perpendicular decline from plateau. However, determining boundary conditions between two cellular regions (such as Core and Invasive edge in Day n spheroids) is less straightforward. Here INSIDIA adopts a method of integrals envisaged as the script outlining a rectangle around the Density-Profile (Figure 1E) with the bottom and left sides of the rectangle fixed along the X and Y axes, respectively, and the top side of the rectangle also fixed, parallel to the X axis and overlaying the plateau region. The right side of the rectangle is then iteratively progressed along the X-axis (at five pixel steps) from the point most distal to the spheroid centre toward the spheroid centre itself (i.e. toward the X-axis origin). The point of intersection of the rectangle with the Density-Profile is identified (Figure 1F) as the core boundary value (i.e. CT (95%)) where the 'area under the curve' for the Density-Profile portion represents at least 95% of the area of the mapped rectangle. Specifically, this CT(95%) value represents a pixel intensity (Figure 1G) later used in Density Map analyses to define an irregular core outline and thus advances the approach of Blacher et al<sup>11</sup>. However, INSIDIA nevertheless retains useful elements of the Blacher et al<sup>11</sup> model, and in a similar manner to these workers defines which of the mapped concentric circular profiles (part of the above 'Density-Profiling') corresponds to the circular delineation of the core boundary, i.e. radius of core.

INSIDIA's approach to determining the core boundary value (CT value) is applicable to any cell type without prior knowledge of invasive behaviour, is independent of

'Spheroid-Segmentation' approach, not influenced by changing background illumination conditions and allows the CT value to be customised to define any target integral, i.e other CT values can be set by the user beyond the default of 95%.

Parameters derived from the 'Density-Profile/Core-Thresholding' step itself include amongst others: the radius of the core (based on a circular profile); average cellular mass of the core and of the invading edge; the maximum length of the invading edge from the core boundary. Details can be found in the INSIDIA Guide.

**3.3 Density Map** (Figure 1H to 1J) utilises the CT value from the above step to delineate an irregular (pixel-intensity driven) core boundary for each spheroid (Figure 1I) which then allows calculation of the physical area of the core and the invasive edge regions. The physical areas (e.g.  $\mu\text{m}^2$ ) are derived from the *a priori* image calibration information, e.g. 1 pixel = 0.3  $\mu\text{m}$ , defined by the user. Like the other stages, a number of secondary parameters can be determined from the 'Density Map' analyses (see INSIDIA Guide.).

### **3.4 Representative results**

Figures 2A and 2B show the four-day (Day 0 to 4) growth and invasion of UP007 glioblastoma cell spheroids within Matrigel ECM and with treatment of the Src/Abl tyrosine-kinase inhibitor, Saracatinib at either 0.5  $\mu\text{M}$  (Figure 2A) or 1  $\mu\text{M}$  (Figure 2B) concentrations. Saracatinib is a recognised inhibitor of invasion in a range of experimental cancer cell lines, including glioblastoma cells<sup>20</sup>. The INSIDIA macro provided quantitative outputs consistent with the qualitative observations including: reduced area of invasive edge when normalised to core perimeter (Figure 2C), reduced maximum length of invasive edge from the core, reduced cellular mass of the invasive edge (Figure 2D). INSIDIA also detected more subtle reductions (reduction of ca. 23-28%) in the core radius at Day 4 compared to Day 0 together with the an increase in the cellular mass of the core across the four-day study period (Figure 2D).

Caveolin-1 (CAV-1) is a protein involved in an array of cell signalling pathways and in Boyden chamber (unpublished studies) in our laboratory CAV-1 appears to be a pro-invasive mediator. Revealing slightly different biology U87MG cells in a 3D spheroid model bearing shRNA CAV-1 knockdown were revealed by INSIDIA to show: (i) significantly reduced spheroid proliferation in the four days of suspension culture prior to the 'Day 0' addition of Matrigel (Figure 2F), an outcome clearly evident from the comparative Day 0 images (Figure 2E); (ii) reductions in the maximum length of



invasive protrusions, and the cellular mass and absolute area of invasive edge (Figure 2H). However, when contextualised against the size of the spheroid itself, i.e. area of the invasive edge normalised to core perimeter (compare Day 2 spheroids in Figure 2E), a reduced CAV-1 status appeared to have no impact (Figure 2G).

The above examples reflect biological change between two time points, however the customisable nature of INSIDIA accommodates analyses of serial images acquired for any individual sphere which represent either multiple time points or indeed serial z-section images.

#### 4 Concluding Remarks

We highlight a customisable open source macro developed on an FIJI<sup>21</sup> platform for the analysis of 3D cancer cell or organoid spheroid invasion assays. The INSIDIA macro is capable of accurate high-throughput high-content analyses providing quantitative parameters of spheroid growth and invasive behaviour. INSIDIA is easily implementable for both fluorescent and bright-field grey images. Future implementations of INSIDIA may involve recognition of collective patterns of invasion<sup>3</sup>.

**Acknowledgements:** MG acknowledges Cancer Research Wales Ed Evans Brain Tumour Scholarship to CM. VP acknowledges EMBL for Bioimage Data analysis course. GP acknowledges the Brain Tumour Research charity.

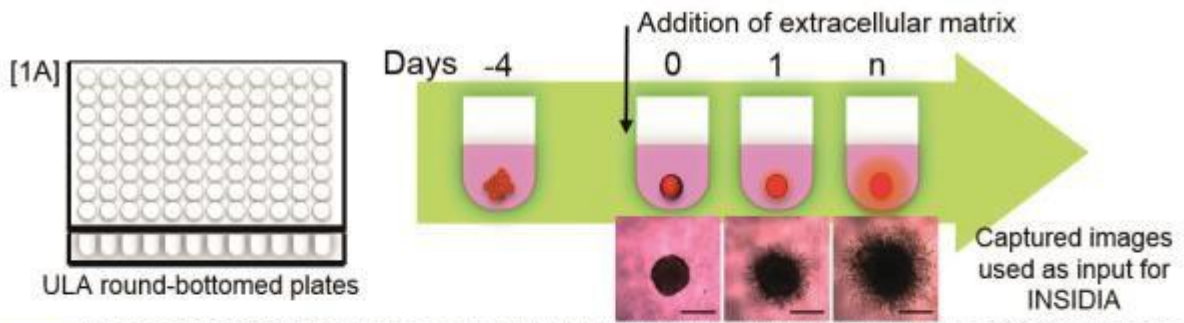
#### References

- 1 Thoma, C. R., Zimmermann, M., Agarkova, I., Kelm, J. M. & Krek, W. 3D cell culture systems modeling tumor growth determinants in cancer target discovery. *Advanced drug delivery reviews* **69**, 29-41 (2014).
- 2 Kramer, N. *et al.* In vitro cell migration and invasion assays. *Mutation Research/Reviews in Mutation Research* **752**, 10-24 (2013).
- 3 Friedl, P., Locker, J., Sahai, E. & Segall, J. E. Classifying collective cancer cell invasion. *Nature cell biology* **14**, 777-783 (2012).
- 4 Vinci, M. *et al.* Advances in establishment and analysis of three-dimensional tumor spheroid-based functional assays for target validation and drug evaluation. *BMC biology* **10**, 1 (2012).
- 5 Vinci, M., Box, C. & Eccles, S. A. Three-dimensional (3D) tumor spheroid invasion assay. *Journal of visualized experiments: JoVE* (2015).
- 6 Friedrich, J., Seidel, C., Ebner, R. & Kunz-Schughart, L. A. Spheroid-based drug screen: considerations and practical approach. *Nature protocols* **4**, 309-324 (2009).
- 7 Solomon, M. A., Lemera, J. & D'Souza, G. G. Development of an in vitro tumor spheroid culture model amenable to high-throughput testing of

- potential anticancer nanotherapeutics. *Journal of liposome research* **26**, 246-260 (2016).
- 8 Naber, H. P., Wiercinska, E., ten Dijke, P. & van Laar, T. Spheroid assay to measure TGF- $\beta$ -induced invasion. *JoVE (Journal of Visualized Experiments)*, e3337-e3337 (2011).
- 9 Stein, A. M., Demuth, T., Mobley, D., Berens, M. & Sander, L. M. A mathematical model of glioblastoma tumor spheroid invasion in a three-dimensional in vitro experiment. *Biophysical journal* **92**, 356-365 (2007).
- 10 De Wever, O. *et al.* Modeling and quantification of cancer cell invasion through collagen type I matrices. *International Journal of Developmental Biology* **54**, 887-896 (2009).
- 11 Blacher, S. *et al.* Cell invasion in the spheroid sprouting assay: a spatial organisation analysis adaptable to cell behaviour. *PloS one* **9**, e97019 (2014).
- 12 Ahammer, H., Helige, C., Dohr, G., Weiss-Fuchs, U. & Juch, H. Fractal dimension of the choriocarcinoma cell invasion front. *Physica D: Nonlinear Phenomena* **237**, 446-453 (2008).
- 13 Jiao, Y. & Torquato, S. Diversity of dynamics and morphologies of invasive solid tumors. *AIP advances* **2**, 011003 (2012).
- 14 Ivanov, D. P. *et al.* Multiplexing spheroid volume, resazurin and acid phosphatase viability assays for high-throughput screening of tumour spheroids and stem cell neurospheres. *PloS one* **9**, e103817 (2014).
- 15 Schindelin, J. *et al.* Fiji: an open-source platform for biological-image analysis. *Nature methods* **9**, 676-682 (2012).
- 16 Palmieri, V. *et al.* Mechanical and structural comparison between primary tumor and lymph node metastasis cells in colorectal cancer. *Soft matter* **11**, 5719-5726 (2015).
- 17 Frangi, A. F., Niessen, W. J., Vincken, K. L. & Viergever, M. A. in *International Conference on Medical Image Computing and Computer-Assisted Intervention*. 130-137 (Springer).
- 18 Singh, H. K., Tomar, S. K. & Maurya, P. K. Thresholding Techniques applied for Segmentation of RGB and multispectral images. *Proceedings published by International Journal of Computer Applications@ (IJCA) ISSN, 0975-8887* (2012).
- 19 Nilufar, S., Morrow, A. A., Lee, J. M. & Perkins, T. J. FiloDetect: automatic detection of filopodia from fluorescence microscopy images. *BMC systems biology* **7**, 66 (2013).
- 20 Ahluwalia, M. S., de Groot, J., Liu, W. M. & Gladson, C. L. Targeting SRC in glioblastoma tumors and brain metastases: rationale and preclinical studies. *Cancer letters* **298**, 139-149 (2010).
- 21 Schindelin, J., Rueden, C. T., Hiner, M. C. & Eliceiri, K. W. The ImageJ ecosystem: An open platform for biomedical image analysis. *Molecular reproduction and development* **82**, 518-529 (2015).

Reference	Geometric Parameters	Isolation of Core and Invasive compartments	Specific Surface (i.e..surface roughness or irregularity)	Open Source Software	Automated/ Semi-Automated Image Processing
Stein 2007 <sup>9</sup>	✓	✓			
Friedrich 2009 <sup>6</sup>	✓		✓		✓
De Wever 2010 <sup>10</sup>	✓		✓	✓	
Naber 2011 <sup>8</sup>	✓				
Vinci 2012 <sup>4</sup>	✓				
Blacher 2014 <sup>11</sup>	✓	✓			✓
Vinci 2015 <sup>5</sup>	✓				
Solomon 2016 <sup>7</sup>	✓				
Ivanov 2014 <sup>14</sup>	✓			✓	✓
INSIDIA	✓	✓	✓	✓	✓

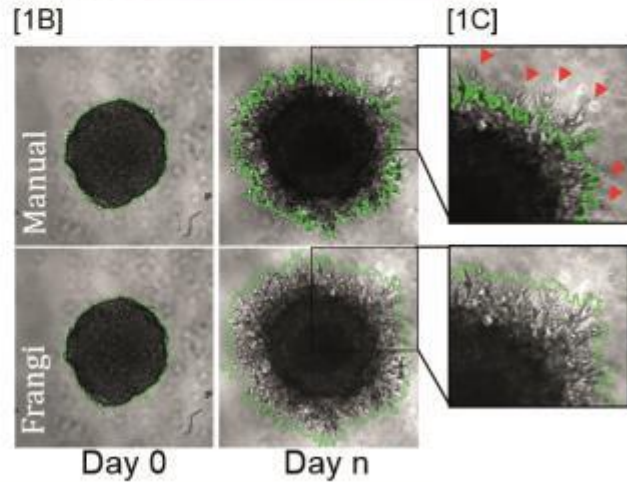
**Table 1** Comparison of INSIDIA features with previously published software algorithms implemented for analysis of 3D spheroids on grayscale images. Parameters that were included in each study are indicated. Geometric Parameters include Spheroid Area, Radius and Volume.



INSIDIA STEPS

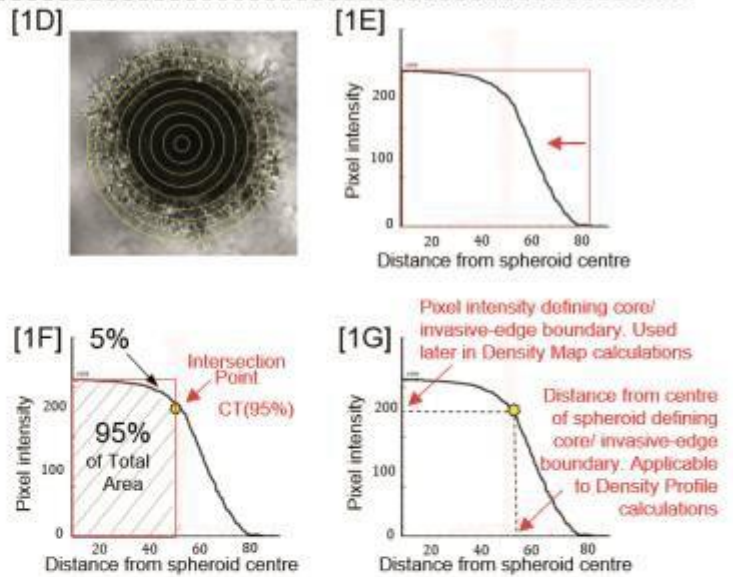
### Spheroid Segmentation

- Defines cellular material from the image background producing a binary image of spheroid outline
- Image-Thresholding or Frangi-Filtering approaches applied according to the image.



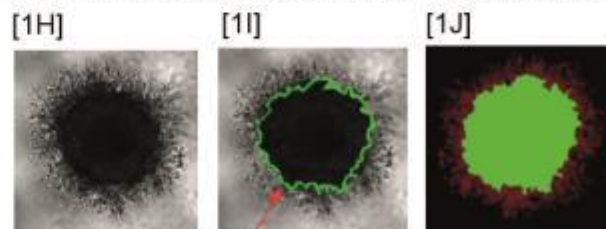
### Density Profile/Core Thresholding

- Defines the spheroid core from cells invading the matrix (Invasive edge).
- Density Profiling determines average pixel density along concentric profiles (1 pixel intervals) starting at the spheroid centre. Profiles are plotted against distance from the spheroid centre
- Core threshold identified by point at which 'area under the curve' of Density Profile represents 95% of the area of a mapped rectangle



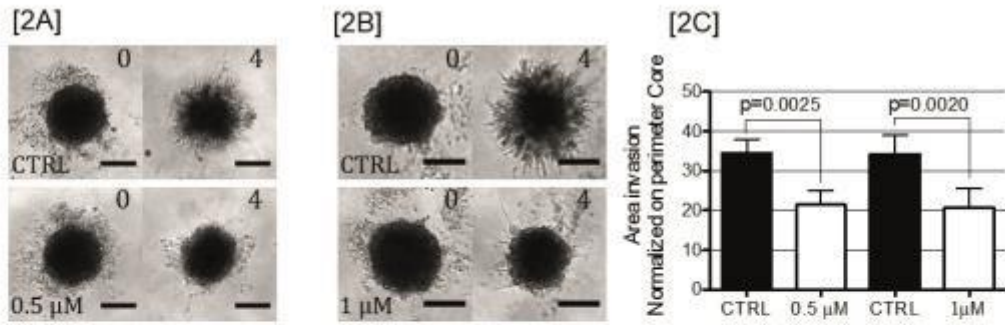
### Density Map

- Determines physical areas (e.g.  $\mu\text{m}^2$ ) in each spheroid for the core and the invasive edge regions.



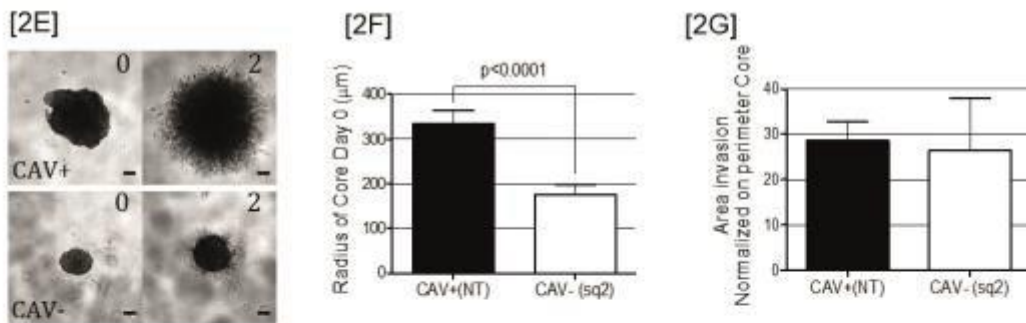
Delineation of irregular core boundary based on Pixel intensity, CT(95%) value, from 'Density-Profile/Core-Thresholding' step.

**FIGURE 1. INSIDIA analysis scheme: Figure 1A Experimental** - Cells seeded as a loose suspended aggregate into 96-well ultra-low-adherence (ULA) plates at, for example, DAY -(minus)4. Subsequently tight spheroidal cell aggregates form, e.g after four days (DAY 0) whereupon the media is replaced with an extracellular matrix. Thereafter time-series images are captured (eg, grey-scale) that illustrate the growth and invasion of the spheroid; **Figures 1B-1C Spheroid-Segmentation** - isolates the spheroid cellular mass from the image background. Accomplished by thresholding the pixel densities as either 'object' or 'background'. The 'Image Thresholding' is determined either automatically or set manually by the user. Where there is poor contrast to background Spheroid-Segmentation may also be accomplished by mathematical modelling using Frangi-Filtering. Figure 1B shows representative images of the same spheroid image analysed by 'Image Thresholding' or 'Frangi-Filtering', immediately upon matrix addition (Day 0) and at the endpoint of the assay (Day n). The green polygon represents a preview of where the segmentation will be applied, the interior of which is identified as 'object' and the exterior as 'background'. Figure 1C shows the respective zoomed images highlighting 'Frangi-Filtering' to better discriminate low contrast cellular material against background. Red arrowheads indicate cellular material which in this example is inappropriately thresholded by the 'Image Thresholding' option. **Figures 1D-1G Density-Profile/Core-Thresholding** - defines the spheroid core from the cellular material invading the surrounding matrix (the 'Invasive edge'). Beginning at the spheroid's geometric centre of mass a series of concentric circular profiles are mapped (Figure 1D). The average pixel density along each circular profile is plotted against the distance from the spheroid's centre to generate a Density-Profile (Figure 1E). To determine the Core boundary INSIDIA adopts a method of integrals 'outlining' a rectangle around the Density-Profile. The right side of the rectangle is then iteratively 'progressed' along the X-axis from the most distal point to inward to the spheroid centre (Figure 1E). The point of intersection at which the area under the curve of the Density-Profile represents 95% of the area of a mapped rectangle (Figure 1F) defines the CT value (95%) i.e. the boundary between core and Invasive edge (Figure 1G). **Figure 1H-1J Density Map** utilises the boundary pixel intensity, the CT value (95%), from 'Density-Profile/Core-Thresholding' to delineate an irregular (pixel-intensity driven) core boundary for each spheroid (Figure 1I) which affords calculation of the Core and Invasive Edge physical areas (e.g.  $\mu\text{m}^2$ ). Figure 1J shows these areas defined by different colours (Green= Core; Red = Invasive Edge).



**[2D]**

Src Inhibitor-Saracatinib (AZD0530) UPO07 cells		CTRL	0.5μM	CTRL	1μM
Day 0	Radius of Core (μm)	137 ±5.59	142 ±3.57	145 ±10.4	142 ±2.56
Day 4 vs Day 0	Day 4 Core Radius as a % relative change to Day 0	-23.1 ±4.39	-23.9 ±5.50	-26.7 ±7.88	-28.5 ±5.04
	Day 4 Core Cellular Mass as a % relative change to Day 0 (μm x pixel intensity)	+17.2 ±9.60	+24.1 ±8.40	+11.7 ±3.72	+20.5 ±7.52
	Day 4 Core Area as a % relative change to Day 0	-26.7 ±8.51	-21.2 ±8.40	-31.4 ±11.8	-27.8 ±8.46
Day 4	Maximum length (μm) of Invasive Edge from Core	140 ±15.9	101* ±20.2	134 ±11.4	94.0* ±12.6
	Cellular Mass of Invasive Edge (μm x pixel intensity)	2648 ±622	1141* ±150	2772 ±341	987* ±184
	Area invasive edges (μm <sup>2</sup> )	36299 ±4214	18362* ±3474	36490 ±2246	15661* ±3976
	Area invasive edges normalized on perimeter Core (μm)	34.5 ±3.47	21.4* ±3.66	34.3 ±4.68	20.7* ±4.88



**[2H]**

Cav-1 lentiviral U87 MG cells		CAV positive (NT)	CAV negative (KD)
Day 0	Radius of Core (μm)	361 ±44.5	201* ±16.5
Day 2 vs Day 0	Day 2 Core Radius as a % relative change to Day 0	+19.9 ±10.8	+13.6 ±10
	Day 2 Core Cellular Mass as a % relative change to Day 0 (μm x pixel intensity)	+58.5 ±72.4	+29.5 ±42.8
	Day 2 Core Area as a % relative change to Day 0	+64.4 ±8.99	+72.4 ±20.4
Day 2	Maximum length (μm) of Invasive Edge from Core	340 ±42.1	231* ±25.9
	Cellular Mass of Invasive Edge (μm x pixel intensity)	11981 ±1425	4888* ±2745
	Area invasive edges (μm <sup>2</sup> )	346609 ±54949	100209* ±15183
	Area invasive edges normalized on perimeter Core (μm)	61.4 ±10.6	49.4 ±18.7

**FIGURE 2. Exemplification of INSIDIA in glioma cell line Invasion. Figures 2A and 2B** - images showing the four-day (Day 0 to 4) growth and invasion of glioma cell UP007 spheroids within Matrigel, in cells treated with vehicle alone (CTRL) or with saracatinib at either 0.5  $\mu$ M (2A) or 1  $\mu$ M (2B) concentrations. Scale bar 150  $\mu$ m; **Figure 2C** - graph showing saracatinib-induced reductions in area of UP007 invasive edge normalised to core perimeter; **Figure 2D** - table showing a selection of parameters derived directly or indirectly from the 'Density-Profile/Core-Thresholding' and Density Map analyses. Statistical analysis \* =  $P < 0.05$  difference between saracatinib treated and control cells; **Figure 2E** - images showing the two-day (Day 0 to 2) growth and invasion of U87MG spheroids within Matrigel, with cells either expressing caveolin-1 (CAV+) or where caveolin-1 was knocked down (CAV-). Scale bar 150  $\mu$ m; **Figure 2E** - graph showing CAV knockdown reduces spheroid proliferation in the four days of suspension culture prior to the 'Day 0' addition of Matrigel, this is clearly evident in the Figure 2E images at Day 0; **Figure 2G** - CAV status has no impact when the area of the invasive edge is normalised to the core perimeter; **Figure 2H** - CAV-1 knockdown-mediated reductions in invasive edge, maximum length of invasive protrusions, and the cellular mass and absolute area of the invasive edge. Statistical analysis \* =  $P < 0.05$  difference between CAV positive and CAV negative cells.